Nexo Revista Científica
Vol. 36, No. 06, pp. 1062-1075/Diciembre 2023

ISSN-E 1995-9516
Universidad Nacional de Ingeniería

http://revistas.uni.edu.ni/index.php/Nexo
https://doi.org/10.5377/nexo.v36i06.17463

Structural and optoelectronic properties of nickel doped CdO thin films deposited by spray pyrolytic technique

Propiedades estructurales y optoelectrónicas de películas delgadas de CdO dopadas con níquel depositadas por técnica de pulverización pirolítica

Abd. F. Haneen *, Khodair T. Ziad, and Al-Dainy. A. Gailan
Department of Physics, College of Science, University of Dyala, Dyala, Iraq
*Corresponding Author: gaaldainy@gmail.com

(recibido/received: 17-agosto-2023; aceptado/accepted: 15-noviembre-2023)

ABSTRACT

In this work, Cadmium oxide (CdO) and Nickle (Ni) doped cadmium oxide (CdO: Ni) thin films have been fabricated onto glass substrate by spray pyrolysis technique. The undoped and Ni-doped CdO thin films have been deposited at 400 °C heated glass substrate. The films' structure, morphology and optical properties were investigated & analyzed as a function of Ni doping level. As confirmed by different characterization, the preparade films have polycrystalline with cubic structure. Based on the results, the pure CdO films showed sharper and more intense diffraction patterns than Ni-doping films. Compared to the pure CdO films, the average grain size of the doped films decreases with increasing of doping level. Furthermore, the optical properties of Ni-doped CdO thin films showed lower absorption coefficient than pure films. However, the higher transparency of Ni-doped CdO films in the visible region consider a good window for the most optoelectronic devices applications. The energy band gap was tuned via Ni doping impurities and it increases as doping level increases.

Keywords: Ni-doped CdO, Spray pyrolysis, thin films, structure properties, transparent film, optoelectronic properties

RESUMEN

En este trabajo, se fabricaron películas delgadas de óxido de cadmio (CdO) y óxido de cadmio dopado con níquel (CdO: Ni) sobre un sustrato de vidrio mediante la técnica de pulverización pirolítica. Las películas de CdO sin dopar y dopadas con Ni se depositaron sobre un sustrato de vidrio calentado a 400 °C. La estructura, morfología y propiedades ópticas de las películas se investigaron y analizaron en función del nivel de dopaje de Ni. Según se confirmó mediante diferentes caracterizaciones, las películas preparadas tienen una estructura policristalina con forma cúbica. Según los resultados, las películas de CdO puro mostraron patrones de difracción más nítidos e intensos que las películas con dopaje de Ni. En comparación con las películas de CdO puro, el tamaño promedio de grano de las películas dopadas disminuye con el aumento del nivel de dopaje. Además, las propiedades ópticas de las películas delgadas de CdO dopado con Ni mostraron un coeficiente de absorción más bajo que las películas puras. Sin embargo, la mayor transparencia de las películas de CdO dopadas con Ni en la región visible se considera una buena ventana para la mayoría de las aplicaciones de dispositivos optoelectrónicos. La banda de energía se ajustó mediante impurezas de dopaje de Ni y aumenta a medida que aumenta el nivel de dopaje.

Palabras claves: CdO dopado con Ni, pulverización pirolítica, películas delgadas, propiedades estructurales, película transparente, propiedades optoelectrónicas

1. INTRODUCTION

Although Transparent conducting oxides (TCOs) have been extensively studied and improved in recent years, combination the transparency, and conductivity in a single material or compound are still challenge for most optoelectronic application (Mohan et al.,2023- Helen et al.,2016). The most common pure TCOs like tin oxide (SnO_2), copper oxide (CuO), and/or zinc oxide (ZnO), were comprehensively studied for their promising and potential applications in optoelectronic devices (Helen et al.,2016- Burbano et al., 2011). CdO-based TCOs received much attention due to unique electronic properties such as high carrier mobilities, nearly metallic conductivity, higher electron mobilities and large carrier concentrations (Burbano et al., 2011- Durmusoglu et al., 2023). CdO is an n-type degenerate semiconductor that has a small indirect band gap (Eg) around 0.84 eV and a larger direct Eg of 2.2 eV (Burbano et al., 2011). Due to high carrier concentrations generated, CdO a noticeable Moss-Burstein shift that leading to extend its Eg depending on the method and/or preparation conditions (Burbano et al., 2011- Durmusoglu et al., 2023). CdO is a simple cubic rock-salt of (FCC) type crystal structure with 4.6483 Å lattice and 1.09 Å ionic reduce. It considers a nonstoichiometric material due to its interstitials and/or oxygen vacancies which is a dominant and intrinsic defect in CdO (Mohan et al.,2023, Burbano et al., 2011- Durmusoglu et al., 2023), As TCOs, CdO was significantly used in various application including photodiodes (Wang et al., 2021), photovoltaic (Wang et al., 2021), detectors (Zhao et al., 2018), gas sensors (Rajput et al.,2019) and as infrared plasmonic material (Runnerstrom et al., 2017). However, as semiconducting thin films CdO relatively poor optical transparency in the short wavelength range (Yang et al., 2005). This drawback property could limit its application as pure TCOs carrier transport layer in planer solar cell and/or light emitted diode architecture. Thus, doping CdO with much smaller ionic radius is still requiring for tuning the optical, structure and electrical properties (Burbano et al., 2011- Durmusoglu et al., 2023).

Nickel impurities of 0.69 Å ionic radius (Pintor-Monroy et al.,2018) was selected in the present work for doping processing to modify the properties of pure CdO. As p-type oxides, Nickel oxide (NiO) is a transition metal oxide with a cubic rock salt structure. It has wide band gap of (3.15-4.3) eV making the material high transparent in the ultraviolet visible and near infrared regions (Li et al., 2023- Napari et al., 2020). In contrast with other common p-type oxides like tin monoxide (SnO), or cuprous oxide (Cu2O), NiO is stable under ambient conditions which makes it ideal materials to solve stability problems and commercial applications (Yan et al., 2001).

Various deposition techniques have been employed to grow undoped CdO and doped CdO-based thin films. These techniques include a physical vapor deposition (Yang et al., 2005, Durmusoglu et al., 2023, Gulino et al.,2002), chemical vapor deposition (Zaho et al., 2002, Matsurra et al., 1997), and chemical-based solution (Saha et al., 2008- Thanachavanont et al., 2011). Based on chemical solution deposition, spray pyrolysis is good approach for growing a uniform and pinhole or crack-free thin films over large areas with controlled thickness. Low fabrication cost and flexible as other advantages to employ spray pyrolysis for thin films deposition (Yan et al., 2001, Vigil et al., 2000, Thanachavanont et al., 2011).

Herein we adopted a spray pyrolysis deposition technique to growth undoped CdO and Ni doping thin films on amorphous glass substrate. The results of Ni doping as small ionic size, showing a significant effect on to the structure, morphological, and optical properties of CdO: Ni - based thin films.

2. EXPERIMENTAL DETAILS

2.1. Material and methods.

All materials in this study were purchased from Thomas Baker and Glentham life sciences and used as received. The source of spray solutions of CdO were prepared using cadmium nitrate tetrahydrate ($Cd(NO_3)_2.4H_2O$) with concentration of (0.2M). The aqueous solution of cadmium nitrate tetrahydrate was prepared at room temperature by dissolving 6.1694 g of the cadmium nitrate tetrahydrate in 100 mL of distilled water, then the solution was constantly stirred for 20 minutes. To prepare the source solutions of NiO, Nickel (II) nitrate hexahydrate ($Ni(NO_3)_2.6H_2O$) with concentration of (0.2M) was used. The solution was prepared at room temperature by dissolving 5.8162g of $Ni(NO_3)_2.6H_2O$ in 100 mL distilled water, then the solutions stirred for 20 minutes.

For doping with NiO, aqueous solution of $Ni(NO_3)_2.6H_2O$ was added to a $Cd(NO_3)_2.4H_2$ aqueous solution with volume ratio of (3, 5, and 7)%. The glass substrates of 2.5 × 2.5 cm were cleaned by sequential sonication in deionized water, and ethanol to remove the organic residues.

The thin films of pure cadmium oxide and/or doped with nickle oxide were prepared by spraying the solutions onto the cleaned glass substrate heated at 400 ºC with air pressure 1.5 bar. The distance between the boat and glass substrate was stet to be 30 cm and the spray rate was controlled by a gas flowmeter at value of 10 ml/min during the spraying process. The heated glass substrates were left to cool at room temperature in ambient air for one day. The average films thickness was measured to be in the range of (300 ± 10) nm for all the prepared samples in this work.

2.2. Material Characterization

The crystalline structures of the prepared thin films were characterized using X-ray diffraction (XRD, Shimadzu X-ray diffraction 6000), The XRD analyzer with Cu K radiation (1.54060 A) at 40 kV and 30 mA. The XRD patterns were recorded for prepared films that deposited onto glass substrate and analyzed from 30° – 80° 2-theta. To study the surface topography of the prepared films, Field Emission- scanning electron microscopy (FE-SEM) (TESCAN- Czech co) was used. Surface morphology of prepend films were measured using atomic force microscopy (AFM) (TT-2, an advanced second-generation tablet microscope -Japan). The tapping mode was applied for different scan sizes. To study the optical properties of prepared films, the transmittance and the absorption spectrum in the wavelength range of (300–900) nm were recorded with a UV−VIS-Spetroscopy double beam spectrophotometer (Visible1900) built by (Sgimadzu, Japanese Co.). Photoluminescence spectrum (PL) of the samples was measured using Shimadzu RF-5301PC model. The PL samples were deposited onto a glass substrate and excited at 325 nm wavelength.

3. RESULTS AND DISCUSSION

3.1 Structural properties of thin films

The XRD patterns at the range of (30°- 80°) 2theta were recorded for doped and undoped films deposited onto the heated glass substrates at 400 ºC in ambient conditions are shown in Figure 1-a. The diffraction peaks at 33º, 38º, 55°, 65°, 69° are clearly visible, which correspond to the reflections from the (111), (200), (220), (311),(222) planes respectively. This finding indicates that the structure of CdO thin films prepared by this method has a polycrystalline structure where the results are in excellent agreement with the (ICDD) card no. (75-0592). No other peaks were observed to indicate an impurity due to high-purity phase was formed. Furthermore, the values of the lattice constants (a) for undoped and Ni-doped CdO prepared thin films were evaluated as shown in table1. It was found that the lattice constants for pure CdO was 4.68378Å with unit cell volume (V) of 102.7 cm^3, which are consistent with the standard from the (ICDD) card no. (75-0592).

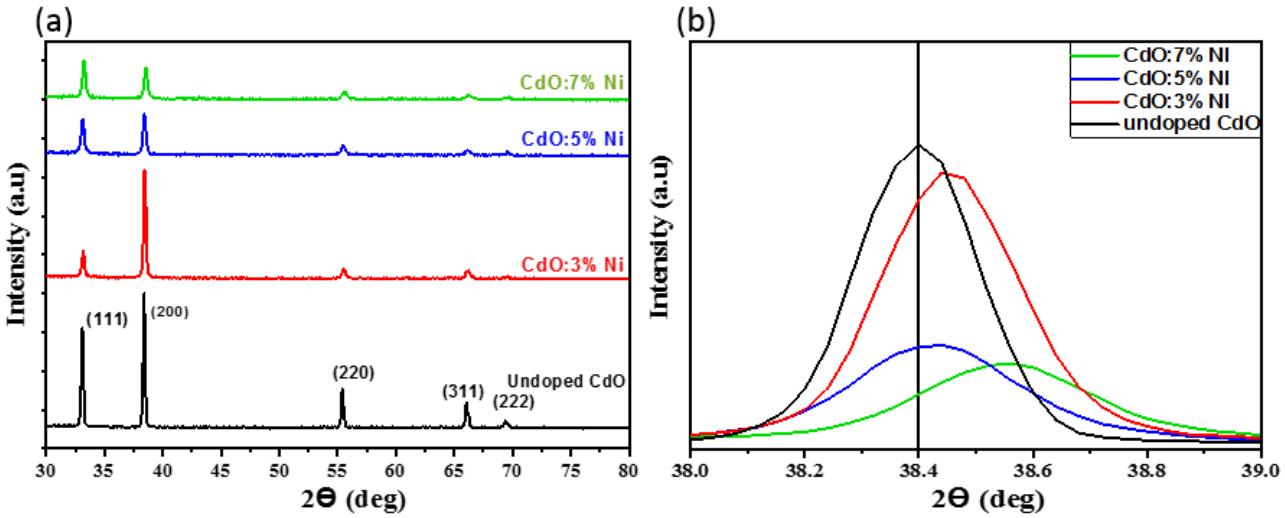

Figur1. (a) XRD pattern for undoped and Ni-doped CdO thin films, and (b) magnified region of the main (200) XRD peak.

As can be seen from figure 1-a, the pure CdO films show sharper and more intense diffraction patterns than Ni-doping films. This finding indicates that the undoped films had better crystalline structures and lattice constant. The magnified region of the main (200) XRD peak at 38.407° for undoped CdO was a slight shift to higher angles upon Ni doping process figure 1-b. The peak shift seen for the Ni doping films resulted from the incorporation of a small Ni ion (radius = 0.69 Å) table 1. Incorporation such Ni ion with larger Cd ion (radius = 1.09 Å) lead to decrease lattice constant of the doping films (Durmusoglu et al., 2023, Thambidurai et al.,2015-Khodair et al.,2019). The average crystallite size (D_{av}) of the films was calculated for the (200) peak using the Scherrer relation (Prabhu et al.,2014).

Table 1. The structure parameters of undoped and Ni-doped CdO thin films.

Sample	(hkl)	Lattice Constant 'a' (Å)	Interplanar Spacing 'd' (Å)	V ($\mathbf{nm^3}$)
CdO:0%**Ni**	200	4.68378	2.34189	102.7
CdO:3%**Ni**	200	4.67772	2.33886	102.3
CdO:5%**Ni**	200	4.6808	2.34040	102.5
CdO:7%**Ni**	200	4.66658	2.33329	101.6

$$D_{av} = \frac{0.9\,\lambda}{\beta \cos\theta} \quad (1)$$

Where β is the full width at half maximum of the (200) peak measured in radians, λ is the used wavelength and θ is the Bragg angle. It was found that the crystallite size covers the range (48 – 28) nm for undoped and Ni-doped CdO thin films, where the size decreases with increasing nickel doping level from 0% to 7% figure 2-a. For further accuracy the crystallite size for the prepared films was also determined using the Williamson–Hall (W– Hall) formula (Ibraheam et al.,2015):

$$\beta_{hkl} \cos\theta = \left(\frac{K\lambda}{D}\right) + 4S \sin\theta \quad (2)$$

where hkl denotes the Miller indices, β_{hkl} is the full width of half maximum of the peak from the (hkl) plane, and (S) is the micro strain in the film. Based on plotted the results of $\beta_{hkl} \cos\theta$ with $4S \sin\theta$ Figure S1 (Supporting Information), the strain and crystallite size can be calculated from the slope and y-intercept of the fitted line

respectively. It was observed that, using the W-Hall formula, the crystallite size as denoted (D_{av} by W– Hall) decreased with increasing the nickle concentration level figure 2-a.

As can be seen from the figure both calculation results of Scherrer and/or W– Hall showed that increase the doping level of nickle ion led to reduce the average crystallite size from approximately 48 nm to 28 nm.

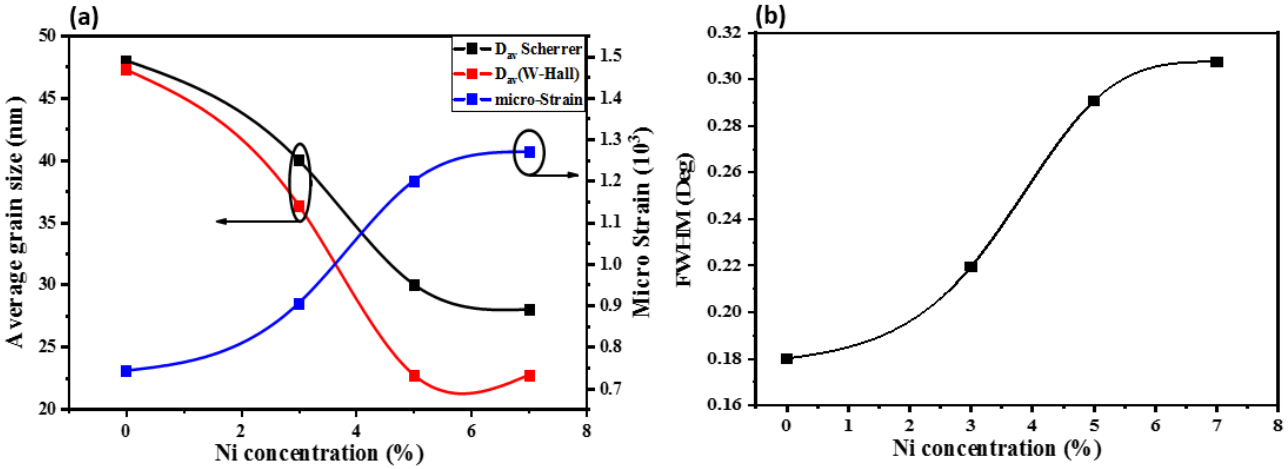

Figure 2. (a) The average grain size and strain as a function of doping concentration, (b) FWHM as function of doping concentration.

Moreover, the strain of CdO crystals was calculated using the following equation (Balu et al., 2015).

$$\xi = \frac{\beta \cos\theta}{4} \tag{3}$$

As mention earlier, the lattice constant of Ni-doped CdO is slightly smaller than that of pure CdO film due to the smaller ionic radius of Ni compared to Cd as presented in table 1 and/or figure S2.

Changes the strain values are mainly occur due to the deformation, defects and/or crystallite size variation, However, it was clearly noted that the strain value of (1–7) % Ni-doped CdO films are lower than the pure CdO films which could be the main point to shift the XRD peaks towards high angle. As can be seen in Figure 2-b, the full width at half maximum (FWHM) of the diffraction peaks at the 200 peaks of pure CdO has been modified due to doping process. The lower value of FWHM indicates a high crystalline and quality films were formed (Khodair et al.,2019).

3.2. Morphological characterizations

The top-view SEM images for pure CdO and Ni-doping films with different concentrations (3, 5, and 7) % have been presented in figure 3. The results showing a uniform, full surface coverage and pinhole free films were formed. Interestingly, different grain sizes were obtained due to Ni doping process. It can be clearly seen that the average grain size (AGS) of deposited films decreases with the increasing the doping concentrations.

The grain size distribution of the prepared films is given in the histogram figure 3. The AGS of undoped CdO film was 97 nm while it was (70, 63, and 46) nm for 3%,5%, and 7% Ni doped respectively. This result was further conformed with the XRD measurements.

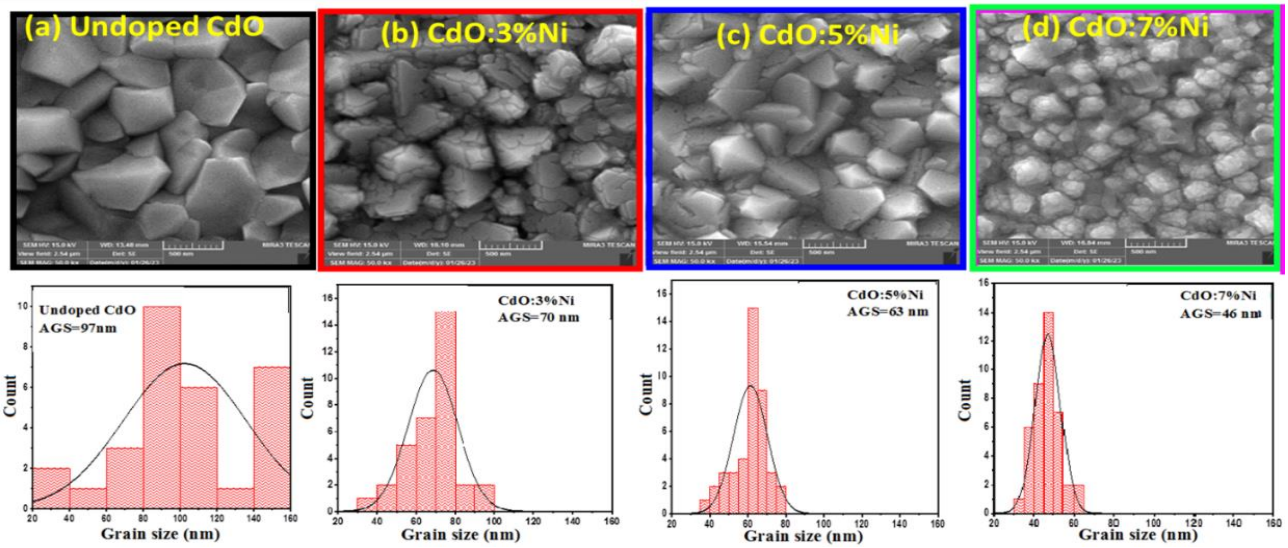

Figure 3. Top-view of SEM images and corresponding statistical grain size for undoped CdO films and Ni-doped CdO thin film**.**

To provide more evidence of the nucleation and growth mechanism of the undoped CdO and Ni-doped thin films, surface roughness and topography of the prepared films were studied using AFM. It was noted from figure 4 that the root mean square (RMS) roughness of the pure CdO films decrease with increasing the nickle doping level over 5.5µm x 5.5µm scan size. The RMS roughness, was (139.5, 10.14, 25.97, and 14.18) nm for pure CdO, CdO:3%NiO, CdO:5%NiO, and CdO:7%NiO films, respectively. Undoped CdO films showed higher voids and cavities on the film surface led to higher RMS roughness surfaces compared to Ni doped films. The AFM results indicate that Ni dopant film have lower particle size compared to undoped CdO film as shown in figure S3. This finding indicated that the films were formed with nanoparticles, where the particle size decrease with the increasing Ni doping level table S1. This result is in agreement with the grain size variation obtained from the XRD results and SEM analyses.

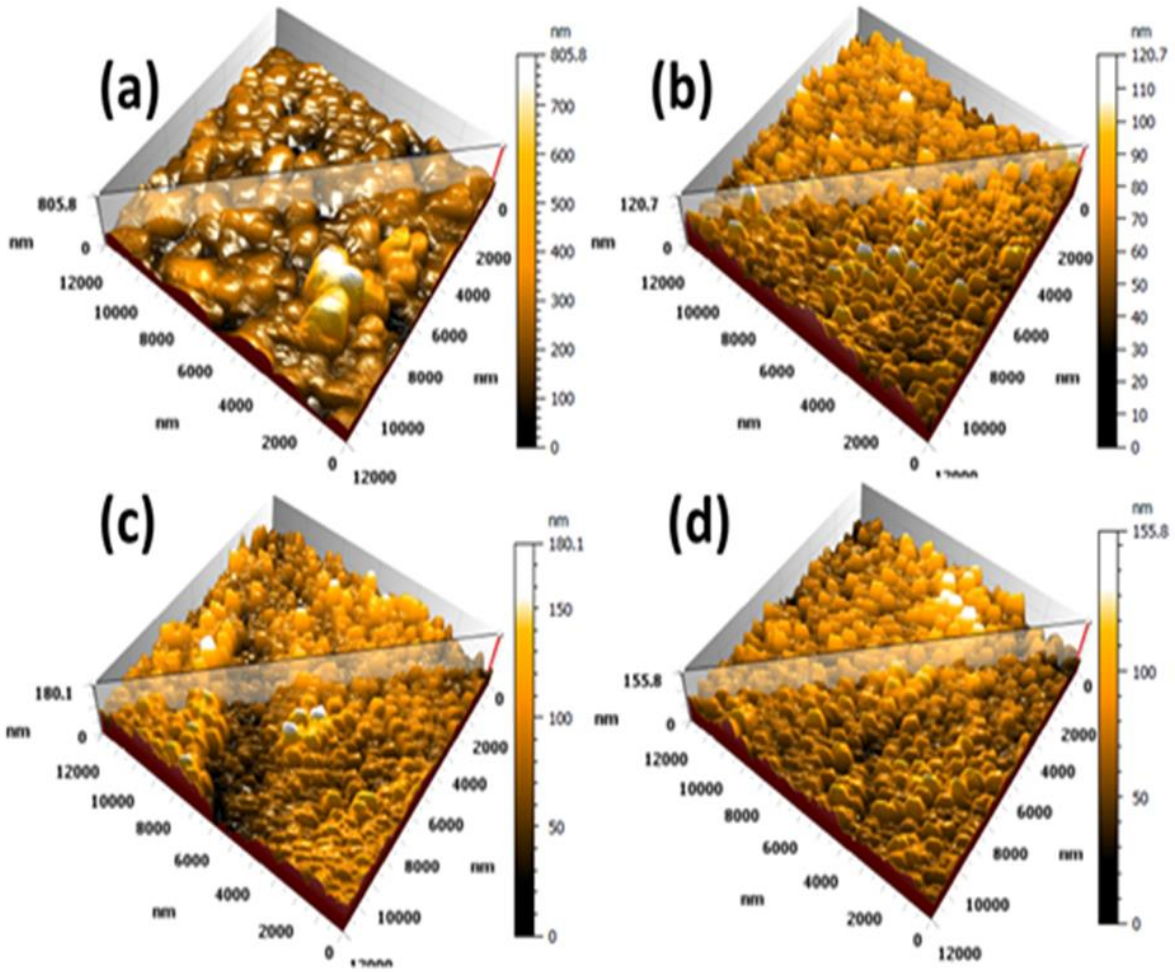

Figure 4. three-dimensional AFM images for Undoped CdO (a), and Ni doped CdO of :3%Ni(b), CdO:5%Ni (c), and CdO:7%Ni(d).

The chemical composition of CdO and Ni doped CdO films have been identified by energy dispersive spectroscopy (EDX) and the results were illustrated in figure 5. As shown in the figure, the undoped CdO films contain only Cd, O and Si peaks. Thus, the doped samples contain Cd, O, Ni and Si peaks. The Ni weight and /or atomic percentage increase as the Ni doping concentration increase. The peak of Si arises from the silica glass of the substrate. Therefore, EDX measurement confirms the presence and compound of expected Ni ions with the CdO thin films.

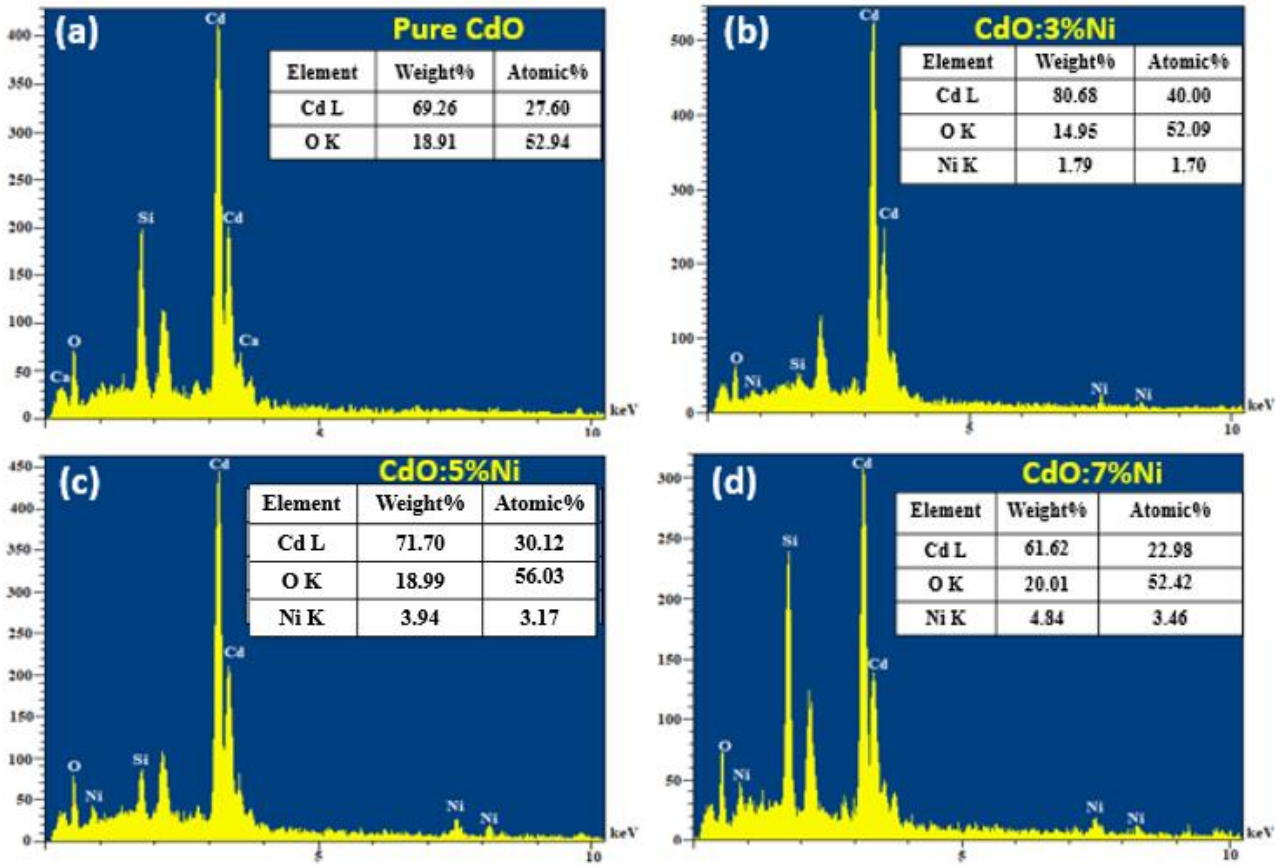

Figure 5. EDS analysis for pure CdO (a) and Ni-doped CdO thin film as: (b) CdO:3%Ni, (c) CdO:5%Ni, and (d) CdO:7%Ni.

3.2 Optoelectronic Properties

In order to gain a broader understanding of doping effects on optical properties, the transmittance and absorbance spectrum of undoped and doping films were recorded as illustrated in figures 5-a and S3. As can be seen, all the prepared films have a good transmittance in the visible region. However, doping pure CdO film with Nickel leading to increase the transmittance over all the wavelength range.

It was found that at 550 nm wavelength, the value of transmittance was 54%, for pure CdO film and it leaps to reach 81% after doping. As can be seen, there is not significant change for transparency at different doping level. Doping CdO with Ni impurity, 28% of transparency was obtain at short wavelength compared to pure CdO films. It can be noted that the absorption of light decreases with increasing the doping level. We believe materials with such transparency is a wide window as carrier transport layer for planer architecture of solar cell. The ability of material to absorb light is measured by its absorption coefficient (α). Thus, (α) can be derived as α = A ln 10/L based on absorption spectrum (A) and sample thickness (L) (AL-Dainy et al., 2020, Humayan et al., 2020). As illustrated in figure (6-b), the values of the absorption coefficient for all prepared films were found to be ($\alpha > 10^4$ cm^{-1}) which is mean that has direct allowed transitions for visible spectra (Thambidurai et al.,2015). It has been shown that absorbance decreases with increasing Ni-doping concentration for the samples at lower wavelength, while its values try to be closer at logger wavelength. Furthermore, the optical energy gap (E_g) of the pure and doped films was estimated using the power law of Tauc (AL-Dainy et al., 2020, Humayan et al., 2020):

$$h\nu = B(h\nu - E_g)^r \quad (4)$$

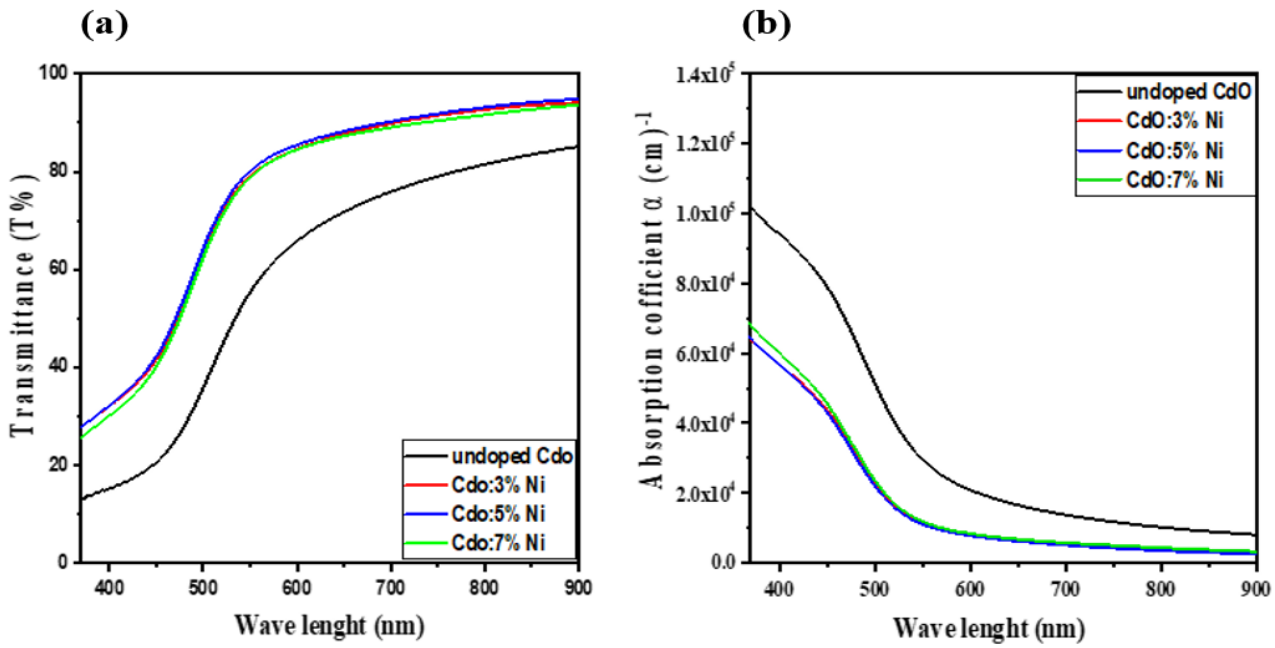

Figure 6. UV−VIS transmittance spectra (a) and Absorption coefficients (b) for undoped and Ni-doped CdO thin films.

where B is a constant and **r** depends on the type of electronic transition. Theoretically **r** is equal to 1/2 for a direct allowed transition (Al-Dainy et al., 2021).

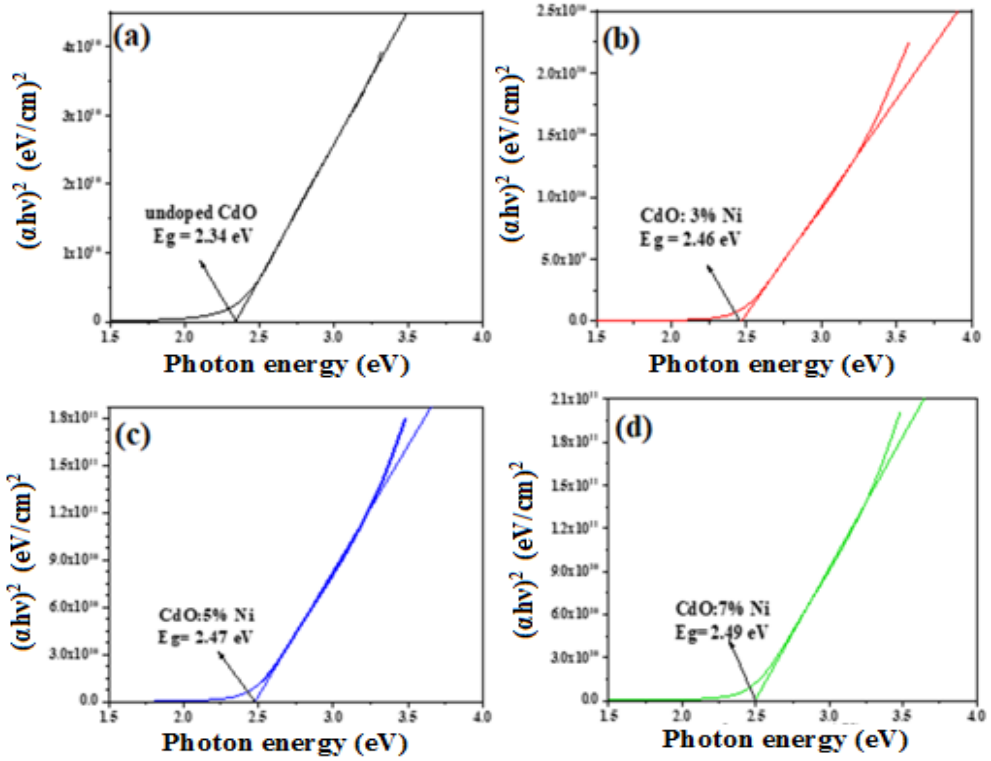

Figure 7. Optical band gap for pure CdO (a), and doped with different Ni concentrations: (b) 3%, (c) 5%, and (d) 7%.

For direct allowed transition, the E_g of the undoped CdO films was 2.34 eV, while it increases with increasing the Ni-doping levels figure 7. As tabulated in table S2, the band gap values were 2.46 eV, 2.47 eV, and 2.49 eV for value increases with increasing Ni-doping concentration in 3%, 5%, and 7% respectively.

Changing the energy band gap by doping process is due to structural modifications of pristine CdO by presence of different defects such as oxygen and /or vacancies interstitials in the doped films (Khodair et al.,2019, Humayan et al., 2021, and Pen et al., 2013). Increasing the band gap of CdO based on Ni doping can be explained by the Mosse–Burstein effect (Burbano et al., 2011, Durmusoglu et al., 2023). The effect refer that a sufficient number of states can be generated due to high carrier concentration by doping process leading to shift the Fermi level toward the conduction band (Velusamy et al., 2015).

The optoelectronic properties of CdO and Ni-doped CdO were further studied by analyzing the steady-state photoluminescence (PL) of the film emission. Based on PL results Figure 8, we are examen the higher energies peak corresponds to excitonic emission at wavelength interval of (450-650) nm for the PL spectra.

As can be seen, a strong peak at 544 nm (2.279 eV) corresponding to the blue green emission of CdO was clearly noted which attributed to near band-edge (Cheemadan et al., 2016-Joshi et al., 2016). The peak energy is approximately close to the energy band gap that estimated from UV-vis spectrum (Serbetci et al., 2020). For Ni doping CdO, the peaks position is shifted towards higher energy (541, 538, and 536) nm based on increasing Ni doping level, The results of peak shifting are due to the impurity and /or surface defects (Nallendran et al., 2018). This finding is approximately consisted with energies band gap calculated from UV-VIS.

The slightly deference in bandgap is probably due to lower crystallization with fewer defects. It has been noted that, the peak intensity for undoped CdO and Ni doping has approximately the same value. However, compared to the previous literature (İskenderoğlu et al., 2019, Serbetci et al., 2020), this work show that pure CdO possessed lower PL intensity due to less recombination rate that could lead to enhance exciton separation efficiency (Nallendran et al., 2018).

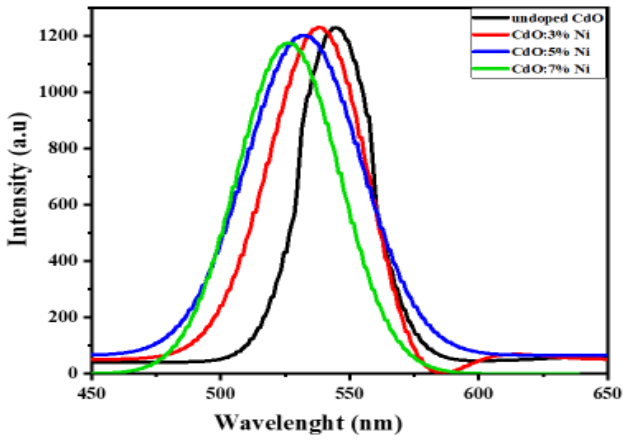

Figure 8. PL intensity against photon wavelength (range500–600 nm) of CdO thin films as a function of different concentration of Ni-doped-CdO.

4. CONCLUSIONS

Pure CdO and nickel doped CdO thin films were synthesized using cadmium nitrate tetrahydrate and nickel (II) nitrate hexahydrate as sources for cadmium and nickel respectively. The undoped CdO and nickel doped CdO thin films have been grown successfully using spray pyrolysis technique. The influence of 0-7% nickel doping level of

CdO on structural, optical and morphological properties of the prepared films were investigated using different characterization. The x-ray diffraction patterns revealed that undoped CdO and Ni-doped films were polycrystalline and exhibit cubic structure. Incorporation Ni ion with larger ionic radius of Cd lead to reduce the lattes constant and grain size.

Reducing grain size for the Ni-doped films was further confirmed via SEM and AFM analyses. The surface morphology based on the SEM results exhibited that, the average grain size of undoped CdO films around 100 nm, while it reduced to less than 40 nm at highest of Ni doping level. As confirmed by AFM, reducing the grain size growth by doping processing led to reduce the surface roughness of the films. Increasing the Ni impurity enhanced the transmittance spectra and the energy band gap of the doping films. However, tuning the optical band gap and enhancing the transmittance spectra though Ni doping is very important for optoelectronic devices applications as carrier transport layer based solar cell.

Acknowledgements

The author and co-authors gratefully acknowledge to the soenore of laboratories at the department of Physics in the collage of scince at Diyala university for providing the necessary facilities to carry out this work.

Funding. This work is a part of MsC. project for Mrs. Haneen F. Abd, and it was not funded by any external agencies.
Competing Interests. There is no conflict of interest about this work because we have not received any funding from any company or university,
Author Contributions. All authors mentioned in the manuscript are contributed to discuss and/or support all the results to build up the manuscript.

ORCID IDs
Haneen F. Abd: https://orcid.org/0009-0007-9703-6163
Ziad T. Khodair: https://orcid.org/0000-0002-5088-0873
Gailan AL-Diany https://orcid.org/0000-0003-0725-5316

REFERENCES

Adhikari, A., Wierzbicka, A., Adamus, Z., Lysak, A., Sybilski, P., Jarosz, D., & Przezdziecka, E. (2023). Correlated carrier transport and optical phenomena in CdO layers grown by plasma-assisted molecular beam epitaxy technique. Thin Solid Films, 780, 139963.

Al-Dainy, G.A. Watanabe, F. Biris, A.S. and Bourdo, S. E. (2021). Surface Passivation of Triple-Cation Perovskite via Organic Halide-Saturated Antisolvent for Inverted Planar Solar Cells. ACS Appl. Energy Mater.4 (4): 3297–3309.

Al-Dainy, G.A. Watanabe, F. Kannarpady, G. K. Ghosh, A. B. Berry, Biris, A.S. and. Bourdo, S. E (2020). Optimizing Lignosulfonic Acid-Grafted Polyaniline as a Hole-Transport Layer for Inverted CH3NH3PbI3 Perovskite Solar Cells. ACS Omega 5 (4): 1887–1901.

Azzaoui, W., Medles, M., Miloua, R., Nakrela, A., Bouzidi, A., Khadraoui, M., ... & Desfeux, R. (2023). Rietveld refinement combined with first-principles study of Zn and Al–Zn doped CdO thin films and their structural, optical and electrical characterisations. Journal of Materials Science: Materials in Electronics, 34(12), 1010.

Balu, A. R. Usharani, K. M. Suganya, and Nagarethinam. V. S. (2015). Cadmium Oxide Thin Films Deposited by a Simplified Spray Pyrolysis Technique for Optoelectronic Applications. Journal of Applied Chemical Research. 47-63. 1,9.

Burbano, M., Scanlon, D. O., & Watson, G. W. (2011). Sources of conductivity and doping limits in CdO from hybrid density functional theory. Journal of the American Chemical Society, 133(38), 15065-15072.

Cheemadan, S. Rafiudeen, A. Kumar, M. S. (2016). Highly transparent conducting CdO thin films by radiofrequency magnetron sputtering for optoelectronic applications. ournal of Nanophotonics, 10, I 3, 033007.

Chen, W. Ma, C. S. Hsieh, Y. Lai, Y. Kuo, C. Chen, S. Chang, Shoou-Jinn Chang, Ray-Hua Horng, and Ying-Hao Chu. (2022). High Stability Flexible Deep-UV Detector Based on All-Oxide Heteroepitaxial Junction. ACS Appl. Electron. Mater., 4 (6), 3099-3106.

Durmusoglu, E. G., Hu, S., Hernandez-Martinez, P. L., Izmir, M., Shabani, F., Guo, M., ... & Demir, H. V. (2023). High external quantum efficiency light-emitting diodes enabled by advanced heterostructures of type-ii nanoplatelets. ACS nano, 17(8), 7636-7644.

Farag, A. A. M., Mohammed, M. I., Ganesh, V., Ali, H. E., Aboraia, A. M., Khairy, Y., ... & Yahia, I. S. (2023). Investigating the influence of Eu-doping on the structural and optical characterization of cadmium oxide thin films. Optik, 281, 170830.

Gulino, A. Dapporto, P. Rossi, P. and Fragalà, I. (2002). A Liquid MOCVD Precursor for Thin Films of CdO. Chem. Mater., 14 (4), 1441-1444 .

Helen, S. J., Devadason, S., & Mahalingam, T. (2016). Improved physical properties of spray pyrolysed Al: CdO nanocrystalline thin films. *Journal of Materials Science: Materials in Electronics*, *27*, 4426-4432.

Humayan, K. M. Hafiz, M. Urmi, S. A. Haque, M. J. Ali, M. M. Rahman, M. S. Khan, M. K.R. and Rahman, M. S. (2022). Effect of Ga Doping on Microstructure, Morphology, Optical and Electrical Properties of Spray Deposited CdO Thin Films. Optical Materials 125, 112123.

Humayan, K. M. Bhattacharjee, A. Islam, M. M. M. S. Rahman, M. Saifur Rahman, and Khan. M. K.R. Effect of Sr Doping on Structural, Morphological, Optical and Electrical Properties of Spray Pyrolized CdO Thin Films. (2021). Journal of Materials Science: Materials in Electronics 32 (3): 3834–42.

Ibraheam, A. S. Al-Douri, Y. Abubaker S. Mohammed, Deo Prakash, Hashim, U. and Verma, K. D. 2015. Electrical, Optical and Structural Properties of Cu2Zn0.8Cd0.2SnS4 Quintern ary Alloy Nanostructures Synthesized by Spin Coating Technique. International Journal of Electrochemical Science 10 (12): 9863–76.

İskenderoğlu, Z. D. (2019). Mg doped CdO thin films grown on glass substrate by spray pyrolysis method. Materials Research Express, 6 026423.

Joshi, S. Ippolito S. J. and Sunkara, M.V. (2016). Convenient architectures of Cu2O/SnO2 type II p–n heterojunctions and their application in visible light catalytic degradation of rhodamine. RSC Advance, 6, 43672-43684.

Kerrigan, M. M. Klesko, J. P. Blakeney, K. J. and Winter, C.H. (2017). Low Temperature, Selective Atomic Layer Deposition of Nickel Metal Thin Films. ACS Appl. Mater. Interfaces, 10, 16,14200–14208.

Khodair, Z. T. Al-Jubbori, M. Hassan, A. M. Aljuboori, M. and Sharrad, F.I. (2019). Structural Properties of (Sn1−xMgxO) Thin Films and Optical Parameter Dependence with Gamma Ray Irradiation. Journal of Electronic Materials 48 (1): 669–78.

Kumari, R., & Kumar, V. (2020). Impact of zinc doping on structural, optical, and electrical properties of CdO films prepared by sol–gel screen printing mechanism. Journal of Sol-Gel Science and Technology, 94, 648-657.

Kumaravel, R., Bhuvaneswari, S., Ramamurthi, K., & Krishnakumar, V. (2012). Structural, optical and electrical properties of molybdenum-doped cadmium oxide thin films prepared by spray pyrolysis method. Applied Physics A, 109, 579-584.

Kwok, C. K. G., & Yu, K. M. (2021). Highly transparent and conducting in doped CdO synthesized by sol-gel solution processing. Journal of Materials Science, 56(22), 12607-12619.

Li, J. Chiang, C. Xia, X. H.Wan, F. Rena and Pearton, S. J. (2023). Superior high temperature performance of 8 kV NiO/Ga2O3 vertical heterojunction rectifiers. J. Mater. Chem. C,,11, 7750-7757.

Matsuura, N., Johnson, D. J., & Amm, D. T. (1997). Fabrication of cadmium oxide thin films using the Langmuir-Blodgett deposition technique. *Thin Solid Films*, *295*(1-2), 260-265.

Mohan, R., Parasuraman, K., Benny Anburaj, D., & Shanmugam, N. (2023). Structural, optical, and electrochemical behaviour for different levels of Ni doped CdO nanoparticles. Journal of Materials Science: Materials in Electronics, 34(8), 712.

Nallendran, R. Selvan, G. and Balu, A. R. (2018.). Photoconductive and Photocatalytic Properties of CdO–NiO Nanocomposite Synthesized by a Cost Effective Chemical Method. Journal of Materials Science: Materials in Electronics 29 (13): 11384–93.

Napari, M. Huq, T. N. Hoye, R. L. Z. MacManus-Driscoll, J. L. (2020). Nickel oxide thin films grown by chemical deposition techniques: Potential and challenges in next-generation rigid and flexible device applications. Info Mat ,3,5, 536-576 .

Pan, L.L. G.Y. Li, Lian, J.S. Structural, optical and electrical properties of cerium and gadolinium films. (2013). Applied Surface Science, 274, 365-370.

Pintor-Monroy, M. I. Barrera, D. Murillo-Borjas, B. L. Ochoa-Estrella, F. J. Hsu, J. W. P. and Quevedo-Lopez, M.A. (2018). Tunable Electrical and Optical Properties of Nickel Oxide (NiOx) Thin Films for Fully Transparent NiOx–Ga2O3 p–n Junction Diodes. ACS Appl. Mater. Interfaces, 10, 44, 38159–38165.

Prabhu, Y.T. Rao, K. V. Kumar, V. S. S. and Kumari, B. S. (2014). X-Ray Analysis by Williamson-Hall and Size-Strain Plot Methods of ZnO Nanoparticles with Fuel Variation. World Journal of Nano Science and Engineering, 04 (01): 21–28.

Rajput JK, Pathak TK, Kumar V, Swart HC, Purohit LP, (2019). Controlled sol-gel synthesis of oxygen sensing CdO: ZnO hexagonal particles for different annealing temperatures. RSC Adv., 2;9(54):31316-31324.

Runnerstrom, E. L. Kelley, K. P. Sachet, E. Shelton, C. T. and Maria, J. (2017). Epsilon-near-Zero Modes and Surface Plasmon Resonance in Fluorine-Doped Cadmium Oxide Thin Films. ACS Photonics, 4 (8) 1885-1892.

Saha, B. Thapa, R. and. Chattopadhyay, K. K (2008). Bandgap Widening in Highly Conducting CdO Thin Film by Ti Incorporation through Radio Frequency Magnetron Sputtering Technique. Solid State Communications 145 (1–2): 33–37.

SERBETCI, (2020). Synthesis and optical properties of uranium- doped cadmium oxide synthesized by sol-gel method. Materials Science-Poland,38(1),23-27.

Thambidurai, M. Muthukumarasamy, N. Ranjitha, A. and Velauthapillai, D. (2015). Structural and Optical Properties of Ga-Doped CdO Nanocrystalline Thin Films. Superlattices and Microstructures 86: 559–63.

Thanachayanont, Chanchana, Visittapong Yordsri, and Chris Boothroyd. (2011). Microstructural Investigation and SnO Nanodefects in Spray-Pyrolyzed SnO2 Thin Films. Materials Letters 65 (17–18): 2610–13.

Velusamy, P. Ramesh Babu, R. Ramamurthi, K. Dahlemc M. S. and Elangovanc, E. (2015). Highly transparent conducting cerium incorporated CdO thin films deposited by a spray pyrolytic technique. RSC Advance ,5, 102741-102749.

Vigil, O. Vaillant, L. Cruz, F. Santana, G. A Morales-Acevedo, Contreras-Puente, G . (2000). Spray pyrolysis deposition of cadmium–zinc oxide thin films. Thin Solid Films, 361–362, 21, 53-55.

Wang, Y., Li, M., Fan, B., Wong, Y. S., Lo, C. Y., Kwok, C. K. G., ... & Yu, K. M. (2021). Flexibility of room-temperature-synthesized amorphous CdO-In2O3 alloy films and their application as transparent conductors in solar cells. ACS Applied Materials & Interfaces, 13(36), 43795-43805.

Yan, M. Lane, M. Kannewurf, C. R. (2001). Highly conductive epitaxial CdO thin films prepared by pulsed laser deposition. Appl. Phys. Lett. 78, 2342–2344.

Yang, Y., Jin, S., Medvedeva, J. E., Ireland, J. R., Metz, A. W., Ni, J., ... & Marks, T. J. (2005). CdO as the archetypical transparent conducting oxide. Systematics of dopant ionic radius and electronic structure effects on charge transport and band structure. Journal of the American Chemical Society, 127(24), 8796-8804.

Zhao, Y., Cui, L., Sun, Y., Zheng, F., & Ke, W. (2018). Ag/CdO NP-engineered magnetic electrochemical aptasensor for prostatic specific antigen detection. ACS applied materials & interfaces, 11(3), 3474-3481.

Zhao, Z. Morel, D. L. and Ferekides, C. S. (2002). Electrical and Optical Properties of Tin-Doped CdO Films Deposited by Atmospheric Metalorganic Chemical Vapor Deposition. Thin Solid Films 413 (1–2): 203–11.